Journal of
Mechanical
Science and
Technology

Journal of Mechanical Science and Technology 21 (2007) 1918~1925

Flow near the corner in buoyant convection in a rectangular cavity

J. S. Park[1,*] and J. M. Hyun[2]

[1]*Department of Mechanical Engineering, Halla University, Wonju, Kangwon-Do, Korea*
[2]*Department of Mechanical Engineering, Korea Advanced Institute of Science and Technology, Daejeon, Korea*

(Manuscript Received May 7, 2007; Revised July 6, 2007; Accepted August 6, 2007)

Abstract

Corner flow, driven by differential heating at the vertical walls in a rectangular cavity, is studied. The flow is initiated from a strong vertical stratification of a Boussinesq fluid. The system Rayleigh number is large and the Prandtl number is O(1). Previous studies point to a considerable thickening of the boundary layer depth, which is referred to as the corner jet when the fluid moves vertically in and horizontally out near the corner. Some authors argue that the phenomenon is caused by an internal hydraulic jump. In some other investigations, the corner jet structure is shown to arise due to the temperature undershoots in the vertical boundary layer, which stem from the stable thermal stratification in the core. In this paper, the above controversy is resolved in part and a theoretical model for the corner flow is given. Furthermore, efforts are made to establish the condition for a smooth turning flow, without abrupt changes of the flow depth, near the corner.

Keywords: Boussinesq fluid; Buoyant convection; International hydraulic jump; Stratification

1. Introduction

Buoyancy-driven convection in an enclosed rectangular cavity constitutes a classical subject. The overall flow and attendant heat transfer under a variety of wall boundary conditions have been extensively documented. One benchmark flow layout is a two-dimensional sidewall-heated rectangular enclosure. Two different temperatures, e.g., T_h and T_c, $\Delta T \equiv T_h - T_c > 0$, are specified, respectively, at the right and left vertical sidewalls. This, in the gravity field, causes a rising (sinking) flow near the right (left) vertical sidewall. The global pattern is characterized by a counter-clockwise circulating flow. At the two horizontal walls, straightforward thermal conditions, such as an insulating wall or an isothermal wall, are often imposed [1-3]. The relevant nondimensional parameters are: the system's Rayleigh number, R_a; the Prandtl number, σ, and the aspect ratio of the cavity, A.

In most technological applications, $R_a >> 1$, and boundary layer-type flow prevails. Thus, flows are concentrated in thin boundary layers adjacent to the walls, and fluid motions are weak in the interior of the cavity. Since the main driving force is the buoyancy generated in the vertical boundary layers, in previous studies, much attention has been given to the vertical boundary layer and the interior. The treatment of the boundary layers on the horizontal walls has been relegated to a subsidiary level [4, 5].

In the standard side-heated cavity model with large R_a, $\sigma \sim O(1)$ and $A \sim O(1)$, the thickness of the vertical boundary layer $O(R_a^{-1/4})$, and the vertical velocity scale $w \sim O(1)$. As mentioned earlier, the vertical boundary layer exerts active control on the entire flow field in the cavity [6]. One important question is the behavior of vertical boundary-layer flow as it approaches the corner region where the vertical wall abuts the horizontal wall. The vertically

*Corresponding author. Tel.: +82 33 760 1219, Fax.: +82 33 760 1211
E-mail address: jspark@halla.ac.kr

directed flow has to negotiate its way in the vicinity of the corner to turn into a horizontally directed flow. Descriptions and physical interpretations of the flow mechanism in the corner region are relatively less numerous and poorly established [7, 8].

In this article, features of the corner flow will be examined by means of theoretical analysis. Of particular interest is the corner flow generated by the singularity of the wall boundary condition. Knowledge of the corner flow will provide an important link in depicting the complete buoyant flow in the entire domain of the cavity. The present effort will also put in perspective some of the earlier arguments on corner flows.

2. Mathematical formulation

An incompressible viscous Boussinesq fluid [kinematic viscosity ν, coefficient of thermal diffusivity κ, coefficient of thermometric expansion α] is contained in a two-dimensional square enclosure [height $2L^*$, width $2D^*$, $L^*/D^* = 2h \sim O(1)$]. The Cartesian coordinates (x,z), together with the corresponding velocity components (u,w) are shown in Fig. 1.

At the basic state, the fluid is motionless with a pre-existing linear stable stratification, i.e., the basic temperature distribution T_r^* in the fluid is given as

$$T_r^* = \frac{1}{2}\left(\left(T_T^* + T_B^*\right) + \left(T_T^* - T_B^*\right)\frac{z^*}{L^*}\right), \tag{1}$$

in which T_T^* and T_B^* denote, respectively, the temperature at the top and bottom walls.

The physical quantities are made dimensionless as follows:

$$\nabla^* = L^*\nabla, \quad p = \frac{p^* - p_r^*}{\varepsilon\rho_0^* g L^* \alpha \Delta T^*}, \quad T = \frac{T^* - T_r^*}{\varepsilon \Delta T^*},$$
$$(u,w) = (u^*, w^*)\sigma^{1/2}/\varepsilon L^* N, \quad t = t^* N \sigma^{1/2}.$$

In the above equations, $\Delta T^* \equiv T_T^* - T_B^*$, superscript * stands for dimensional quantities, subscript r refers to the basic state reference conditions, and subscript 0 denotes the values at the origin (x=z=0). The strength of perturbation is gauged by ε, which is assumed to be small $(\varepsilon << 1)$, N and σ are respectively the Brunt-Vaisala frequency $N = (\alpha g \Delta T^*/L^*)^{1/2}$ and the Prandtl number $\sigma = \nu/\kappa$.

Neglecting the terms of $O(\varepsilon)$, the steady-state linearized governing equations, in non-dimensional form, are

$$\frac{\partial u}{\partial x} + \frac{\partial w}{\partial z} = 0, \tag{2}$$

$$-\frac{\partial p}{\partial x} + R_a^{-1/2}\left(\frac{\partial^2 u}{\partial x^2} + \frac{\partial^2 u}{\partial z^2}\right) = 0, \tag{3}$$

$$-\frac{\partial p}{\partial z} + T + R_a^{-1/2}\left(\frac{\partial^2 w}{\partial x^2} + \frac{\partial^2 w}{\partial z^2}\right) = 0, \tag{4}$$

$$-w + R_a^{-1/2}\left(\frac{\partial^2 T}{\partial x^2} + \frac{\partial^2 T}{\partial z^2}\right) = 0. \tag{5}$$

In the above, R_a denotes the Rayleigh number $R_a = \alpha g \Delta T^* L^{*3}/\nu\kappa$, which is assumed to be very large, i.e., $R_a >> 1$.

The associated boundary conditions are set as follows. At the top and bottom horizontal walls, the basic-state isothermal conditions are unperturbed, i.e.,

$$T = 0, \; u = w = 0 \quad \text{at} \quad z = \pm 1. \tag{6a}$$

At right (left) vertical wall, the temperature perturbation of unit strength is imposed as $T = +1$ $(T = -1)$ except in the localized corner area of length δ. The boundary condition near the corner is dealt with by introducing a function of $z-$ corner zone near the horizontal wall. Wall thermal condition at the vertical wall near the corner zone is assumed a function of the z-coordinate:

$$u = w = 0, T = \pm f(z) \text{ at } x = \pm 1 \tag{6b}$$

in which $f(z) = \pm 1$ at $|z| \le 1 - \delta$,
and, in the $z-$ region $1 - \delta < |z| \le 1$,
the function $f(z)$ varies between $f(|z| = 1) = 0$
and $f(|z| = 1 - \delta) = 1$.

In the case of $\delta \neq 0$, the above thermal variation by $f(z)$ could effectively remove a mathematical singularity due to an abrupt jump-discontinuity at the corner point when $\delta = 0$, i.e., horizontal and vertical walls meet at different temperatures of $T_{HW} = 0$ and $T_{VW} = 1$ or -1. Herein, δ is assumed to be very small positive value: $\delta \sim O(R_a^{-1/6}) << 1$. Evidently, if $\delta = 0$, a discontinuity in the wall temperatures at the

corner, i.e., $T_{HW}=0$ and $T_{VW}=1$ or -1, is seen, in which subscripts HW and VW denote, respectively, horizontal and vertical wall. The above formulation with $\delta \neq 0$ is set up to handle this mathematical singularity, and δ is assumed to be very small: $\delta \sim O(R_a^{-1/6}) << 1$. The proper size of δ as well as the function $f(z)$ will be determined in the subsequent analysis based on the consideration of smooth-turning condition in the vicinity of the corner. In passing, it is mentioned that a formulation with $\delta \neq 0$ leads to a model to effectively describe the realistic systems.

3. Analysis

For $R_a >> 1$, as sketched in Fig. 1, the flow field can be divided into the inviscid interior (I), buoyancy layer near the vertical wall (II), horizontal boundary layer on the horizontal wall (III) and the corner regions where the horizontal and vertical boundary layers meet (IV). To secure the solution, a flow variable Φ is written as $\Phi = \Phi_i + \Phi_{vb} + \Phi_{hb} + \Phi_c$, and the boundary layer matching technique will be deployed, where subscripts i, vb, hb, c refer, respectively, to the above-referenced regions I, II, III and IV [9].

3.1 Interior flow

Let's consider the interior solution by neglecting the viscous diffusion terms in Eqs. (3)-(5). From Eq. (3), the pressure is a function of z only; thus, the temperature field also becomes a function of z only [see Eq. (4)]. Therefore, the interior temperature should be

$$T_i = 0 . \tag{7}$$

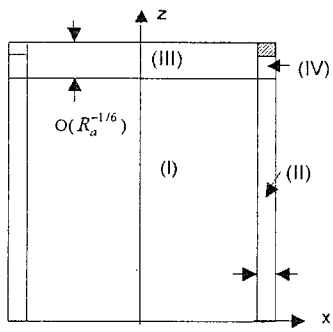

Fig. 1. Configuration of the flow field.

It is noted that the temperature field is anti-symmetric about $x=0$, which stems from the problem definition. From Eqs. (2) and (5), interior velocities are

$$u_i = w_i = 0 . \tag{8}$$

As a result, the leading-order interior variables are the same as those of basic state, i.e., the interior fluid is in the state of motionless linearly stable temperature distribution of Eq. (1).

3.2 Vertical boundary layer flow

Next, consider the vertical boundary layer. By expanding the vertical boundary layer variables into a Taylor-series with the expansion-parameter of $R_a^{-1/4}$, $\Phi_h = \sum_{n=0}^{\infty} R_a^{-n/4} \Phi_h^n$, in which $\Phi \sim u, w, T \text{ or } p$. The leading order flow variables are properly scaled as

$$u_{vb} = R_a^{-1/2}\bar{u}_{vb}, w_{vb} = \bar{w}_{vb}, T_{vb} = \bar{T}_{vb}, p_{vb} = R_a^{-1/2}\bar{p}_{vb} .$$

One obtains the corresponding boundary layer variables $\eta_j = R_a^{1/4}(1+(-1)^j x)$, where $(j=0,1)$ refer, respectively, to the left and right vertical boundary layer coordinates. Substituting the above relations into Eqs. (2)-(5), together with the boundary condition, the leading-order vertical boundary layer equations are

$$\bar{T}_{vb} + \partial^2 \bar{w}_{vb} / \partial \eta_j^2 = 0, \tag{9}$$

$$\bar{w}_{vb} = \partial^2 \bar{T}_{vb} / \partial \eta_j^2 , \tag{10}$$

which are subject to the boundary conditions

$$\bar{T}_{vb} = (-1)^{j+1},\ \bar{w}_{vb} = 0 \quad \text{at} \quad \eta_j = 0,\ (j=0,1), \tag{11a}$$

$$\text{and} \quad \bar{T}_{vb} = \bar{w}_{vb} = 0 \quad \text{as} \quad \eta_j \to \infty . \tag{11b}$$

The boundary layer solutions are

$$\bar{T}_{vb} = (-1)^{j+1} \exp(-\eta_j/\sqrt{2}) \cos(\eta_j/\sqrt{2}), \tag{12a}$$

$$\bar{w}_{vb} = (-1)^{j+1} \exp(-\eta_j/\sqrt{2}) \sin(\eta_j/\sqrt{2}) . \tag{12b}$$

3.3 Horizontal boundary layer flow

Since the problem is symmetric about the mid-height, only the boundary layer flow near the top

horizontal wall ($z=1.0$) is treated. For the top horizontal layer, introducing the stretched vertical coordinate $\zeta=(1-z)R_a^{1/6}$, and using the expansion parameter $R_a^{-1/12}$, the meaningful scaling of horizontal layer variables is given:

$$u_{hb}=R_a^{-1/12}\bar{u}_{hb},\ w_{hb}=R_a^{-1/4}\bar{w}_{hb},$$
$$T_{hb}=R_a^{-1/12}\bar{T}_{hb},\ p_{hb}=R_a^{-1/4}\bar{p}_{hb}.$$

Placing the above scaled variables into the governing Eqs. (2)-(5) yields

$$\frac{\partial\bar{u}_{hb}}{\partial x}-\frac{\partial\bar{w}_{hb}}{\partial\zeta}=0, \tag{13}$$

$$-\frac{\partial\bar{p}_{hb}}{\partial x}+\frac{\partial^2\bar{u}_{hb}}{\partial\zeta^2}=0, \tag{14}$$

$$\frac{\partial\bar{p}_{hb}}{\partial\zeta}+\bar{T}_{hb}=0, \tag{15}$$

$$\bar{w}_{hb}=\frac{\partial^2\bar{T}_{hb}}{\partial\zeta^2}, \tag{16}$$

with the associated boundary conditions,

$$\text{at } \zeta=0,\ \bar{u}_{hb}=\bar{w}_{hb}=\bar{T}_{hb}=0, \tag{17a}$$
$$\text{at } x=\pm1,\ \bar{u}_{hb}=-1/\sqrt{2}\cdot df(\zeta)/d\zeta, \tag{17b}$$
$$\text{as } \zeta\to\infty,\ \bar{u}_{hb},\ \bar{w}_{hb},\ \bar{T}_{hb}\to0. \tag{17c}$$

The boundary condition (17b), related to the fluid transport from the left-wall vertical boundary layer to the right-wall boundary layer, is obtained from the corner zone analysis in the next section.

For the solutions of Eqs. (13)-(16), in view of anti-symmetric character of $\bar{w}_{hb}$ and Eq. (17b) for $\bar{u}_{hb}$, one has

$$\bar{w}_{hb}=\sum_{k=0}^{\infty}g_k(\zeta)\sin\frac{(2k+1)}{2}\pi x, \tag{18}$$

$$\bar{u}_{hb}=A(\zeta)-\sum_{k=0}^{\infty}\frac{2}{(2k+1)\pi}g_k^{(1)}(\zeta)\cos\frac{(2k+1)}{2}\pi x, \tag{19}$$

$$\bar{T}_{hb}=-A^{(1)}(\zeta)x+\sum_{k=0}^{\infty}\left(\frac{2}{(2k+1)\pi}\right)^2 g_k^{(4)}(\zeta)\sin\frac{(2k+1)}{2}\pi x, \tag{20}$$

in which $A(\zeta)=-\frac{1}{\sqrt{2}}\frac{df(\zeta)}{d\zeta}$.

Substituting Eqs. (18)-(19) into Eqs. (13)-(16) and after some mathematical manipulations, one has the equation for $g_k(\zeta)$:

$$g_k^{(6)}-\lambda_k^6 g_k=(-1)^k 2A^{(5)} \tag{21}$$

in which $\lambda_k=((2k+1)\pi/2)^{1/3}$, and the boundary conditions are

$$g_k(0)=0,\ g_k^{(1)}(0)=(-1)^k 4A(0)/(2k+1)\pi,$$
$$g_k^{(4)}(0)=(-1)^k 2A^{(3)}(0). \tag{22}$$

To solve the above Eq. (21), without loss of generality, it may be assumed that $f(\zeta)=(1-\exp(-\alpha\zeta))$ where $\alpha\sim(1)$. Then, the solution for g_k can be obtained in a straightforward manner but the results are omitted here.

3.4 Corner flow

For the left and right extension regions (IV) of size ($R_a^{-1/4}\times R_a^{-1/6}$) near the top wall, the stretched coordinates are $\eta_j=R_a^{1/4}(1+(-1)^j x)$, ($j=0,1$ denote, respectively, the left and right corner), and $\zeta=R_a^{1/6}(1-z)$. The meaningful scales for corner variables are

$$u_c=R_a^{-1/12}\bar{u}_c,\ w_c=\bar{w}_c,$$
$$T_c=\bar{T}_c,\ p_c=R_a^{-1/3}\bar{p}_c.$$

Substituting the above variables into Eqs. (2)-(5) yields

$$(-1)^j\frac{\partial\bar{u}_c}{\partial\eta_j}-\frac{\partial\bar{w}_c}{\partial\zeta}=0, \tag{23}$$

$$\bar{T}_c+\frac{\partial^2\bar{w}_c}{\partial\eta_j^2}=0, \tag{24}$$

$$\bar{w}_c-\frac{\partial^2\bar{T}_c}{\partial\eta_j^2}=0, \tag{25}$$

together with the boundary conditions

$$\bar{u}_{hb}(x\to(-1)^{j+1},\zeta)+\bar{u}_c(\eta_j\to0,\zeta)=0, \tag{26a}$$
$$\bar{w}_c(\eta_j\to0,\zeta)=0, \tag{26b}$$
$$\bar{T}_c(\eta_j\to0,\zeta)=(-1)^j(1-f(\zeta)), \tag{26c}$$
$$\text{and, as } \eta_j\to\infty \text{ or } \zeta\to\infty,\ \bar{u}_c,\ \bar{w}_c,\ \bar{T}_c\to0. \tag{26d}$$

The solutions to the above are found from Eqs. (24) and (25):

$$\bar{T}_c = (-1)^j (1 - f(\zeta)) \exp(-\eta_j / \sqrt{2}) \cos(\eta_j / \sqrt{2}), \quad (27)$$

$$\bar{w}_c = (-1)^j (1 - f(\zeta)) \exp(-\eta_j / \sqrt{2}) \sin(\eta_j / \sqrt{2}), \quad (28)$$

and by integrating Eq. (23),

$$\bar{u}_c = \frac{1}{\sqrt{2}} \frac{df(\zeta)}{d\zeta} \exp\left(-\frac{\eta_j}{\sqrt{2}}\right)\left(\sin\left(\frac{\eta_j}{\sqrt{2}}\right) + \cos\left(\frac{\eta_j}{\sqrt{2}}\right)\right). \quad (29)$$

Combining Eqs. (26a) and (29), the compatibility condition for mass transport between the horizontal layer and the ($R_a^{-1/4} \times R_a^{-1/6}$) corner region is secured

$$\bar{u}_{hb} = -\frac{1}{\sqrt{2}} \frac{df(\zeta)}{d\zeta}. \quad (30)$$

Equation (30) was already utilized to a boundary condition at $x = \pm 1$ to solve the horizontal layer flow [see Eq.(12b)].

4. Result and discussion

Exemplary plots of analytic solution obtained in the previous section are shown in Figs. 2(A)-(C), for

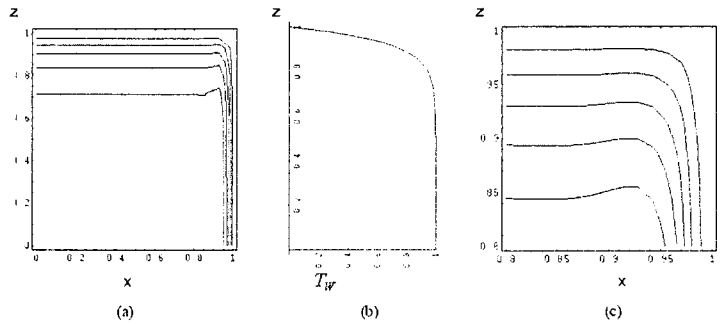

Fig. 2(A). Plots of the streamlines at $R_a = 10^7$ and $\alpha = 0.5$. $T_{HW} = 1 - \exp[-\alpha(1-z)R_a^{1/6}]$
(a) Global streamlines in the 1/4 region, (b) Wall temperature, T_{HW} along the vertical wall, (c) Local streamlines neat the corner.

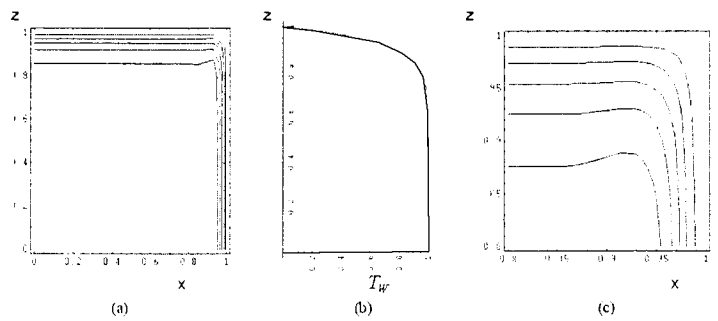

Fig. 2(B). The same as Fig. 2(a) except $\alpha = 1.0$.

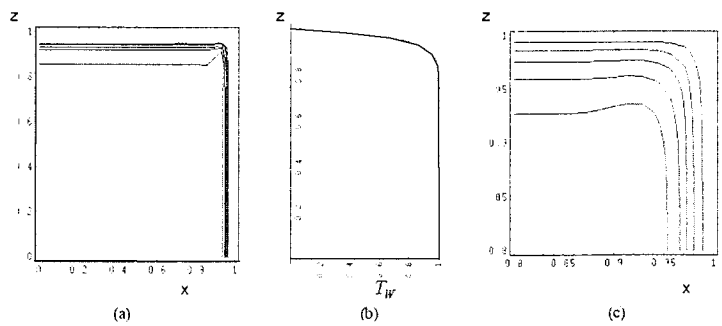

Fig. 2(C). The same as fig. 2(A) except $\alpha = 2.0$.

which the thermal boundary conditions are defined as, at the horizontal walls, $T_{HW}=0$ and at the vertical walls,

$$T_{VW}=(-1)^{j+1}\left(1-\exp[-\alpha(1-|z|)R_a^{1/6}]\right), \qquad (31)$$

where $j=0(\textit{left wall})$ and $j=1(\textit{right wall})$. The system Rayleigh number is fixed as $R_a=10^7$. For each of the cases of Fig. 2, column (A) denotes a plot of streamlines in the first quadrant of global flow-field region and column (C) is a local magnification plot near the corner. Column (b) denotes a wall temperature condition corresponding to each case along the vertical wall for the cases of each column (A) & (C) in Figs. 2(A)-(C).

Figs. 2(A)-(C) show that as the value of α increases, the thickness of horizontal boundary layer, λ, decreases while the flow turns around the corner region ($R_a^{-1/4}\times R_a^{-1/6}$), i.e., region IV in Fig. 1. Those are clearly seen also in Fig. 3.

Taking look at flow physics in region IV, the fluid gradually changes its direction from vertically upward incoming-direction to horizontally leftward departing-direction by the action of buoyancy force imposed by the temperature difference between unperturbed basic interior temperature, T_I and vertical wall temperature, T_{VW} at the same $z-$location, i.e., $\Delta T=T_{VW}-T_I$.

Meanwhile, it is noted that a constant, α, plays a role as a scale factor on $z-$variation of function T_{VW} when the vertical wall temperature matches the horizontal wall temperature [see Eq. (31)]. The larger α-value renders the shorter $z-$varying length scale of vertical wall temperature, T_W [see Eq. (31)]. Up-rising fluid along the vertical layer is set in motion with a constant velocity in region II, which is induced by the buoyancy force owing to $\Delta T=1.0$. The up-rising fluid, however, begins to decelerate in the region IV, i.e., $|1-z|\sim O(\alpha^{-1}R_a^{-1/6})$ where $\Delta T<1.0$ [see Fig. 1 & Eq. (31)]. A critical location z_C, which is a beginning point of deceleration of the fluid upward motion, may be specified as $z_C\approx 1-\alpha^{-1}R_a^{-1/6}$. Thus, the above defined variable z_C has a meaning of distance for up-rising fluid to undergo a certain deceleration while the fluid is traveling along the vertical boundary layer.

In the limit of $\alpha\to\infty$, the beginning point of deceleration approaches $z_C\to 1.0$, which means, from the point of scale analysis, the uprising fluid doesn't turn around in the ($R_a^{-1/4}\times R_a^{-1/6}$) corner region but it must go around the corner through the ($R_a^{-1/4}\times R_a^{-1/4}$) corner region, i.e., a hatched tiny region in Fig. 1. The width of fluid passage is $O(R_a^{-1/4})$ in the zone just after the turning, but it is noted that the width of the horizontal layer away from the corner should be $O(R_a^{-1/6})$ in region III in Fig. 1. As a result, in the case when there is a jump discontinuity in wall temperature at the corner without a matching zone, i.e., $T(x=\pm 1,z)=1.0$, the resultant flow shows a jet-like pattern due to a sudden expansion of flow area after turning to approach the horizontal layer of thickness of $O(R_a^{-1/6})$ [see Fig. 1].

However, if the vertical wall-temperature changes gradually into the horizontal wall temperature along the vertical wall over a length of $|1-z|\sim O(R_a^{-1/6})$ near the corner, it could provide, over a relatively long distance, a wall temperature-matching zone [region IV in Fig.1] for adaptively smooth turning by buoyancy force reducing, which, in turn, makes a retardation of fluid vertical velocity. This allows a smooth turning in the region ($R_a^{-1/4}\times R_a^{-1/6}$).

Fig. 4 shows a schematic plot on the above argument.

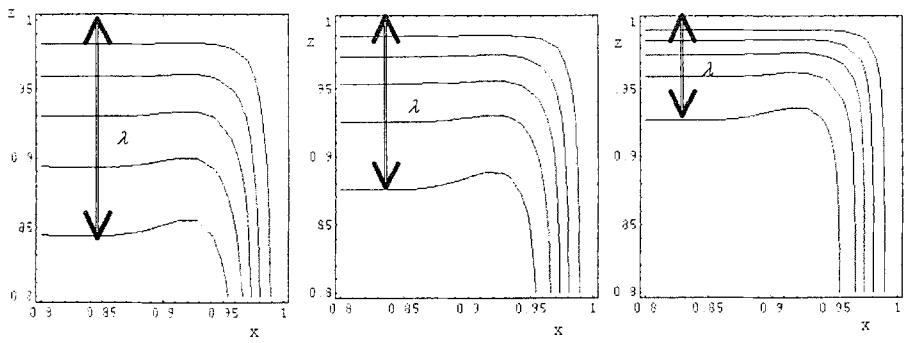

Fig. 3 Comparison of the streamline patterns. $R_a=10^7$ (a) $\alpha=0.5$; (b) $\alpha=1.0$; (c) $\alpha=2.0$.

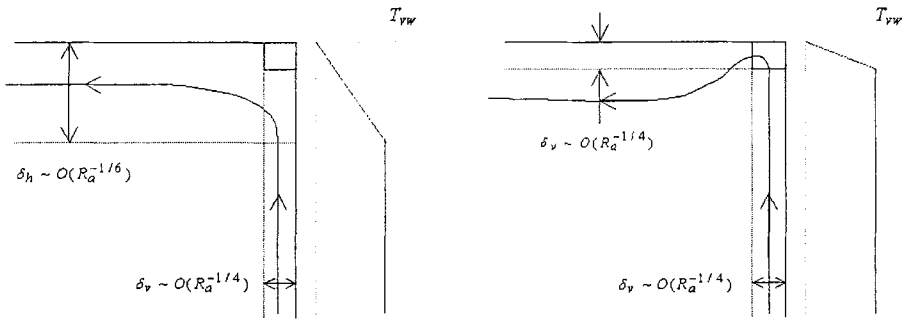

Fig. 4. Schematics of flow pattern. The length scales of z – variation of vertical wall temperature, T_{vw}, are : (a), O($R_a^{-1/6}$); (b), $O(R_a^{-1/4})$.

5. Concluding remarks

In the previous analysis, an analytic solution was obtained by the boundary layer matching method. The solution shows that, if the thermal condition at the vertical wall varies gradually over the length scale of $|1-z| \sim O(R_a^{-1/6})$ near the corner to match the temperatures between horizontal and vertical walls, the corner flow turns smoothly around. In that case, the fluid is moving upward from buoyancy layer at the right vertical wall, turning in the ($R_a^{-1/4} \times R_a^{-1/6}$) corner region and being ejected horizontally out along the horizontal boundary layer near the top wall [see Fig. 1].

However, in the case when there is a jump discontinuity in wall temperature at the corner without a matching zone, i.e., $T(x=\pm 1, z)=1.0$ over $-1 \le z \le 1$, the flow can no longer make a smooth turning. The rising flow along the right vertical wall cannot turn around in the region of ($R_a^{-1/4} \times R_a^{-1/6}$). A smooth turning can be made in the region of ($R_a^{-1/4} \times R_a^{-1/4}$). This is based on the compatibility condition [Eq.(30)]. The resultant flow shows a jet-like pattern due to a sudden expansion of flow area after turning to approach the horizontal layer of thickness of $O(R_a^{-1/6})$ [see Fig. 1].

Physically speaking, consider the wall-temperature decreasing along the vertical wall in the region, $|1-z| \sim O(R_a^{-1/6})$, near the corner. This weakens the vertical buoyancy force which, in turn, makes a retardation of fluid vertical velocity. This allows a smooth turning. On the other hand, if there is no wall temperature-matching zone, the flow lacks a decelerating mechanism in the vertical boundary layer of ($R_a^{-1/4} \times R_a^{-1/6}$) region. The fluid goes up to the region ($R_a^{-1/4} \times R_a^{-1/4}$) without any turning motion while passing the region ($R_a^{-1/4} \times R_a^{-1/6}$). The width of fluid passage is $O(R_a^{-1/4})$ in the zone just after the turning, but it is $O(R_a^{-1/6})$ in the horizontal layer away from the corner. Thus, a corner-jet like motion occurs, which is brought forth from the singularity of thermal wall boundary condition at the corner point.

Acknowledgement

"This work was supported by the Korea Research Foundation Grant funded by the Korean Government (MOEHRD)" (KRF-2005-042-D00041).

References

[1] G. De Vahl Davis and I. P. Jones, Natural convection of air in a square m cavity : a comparison exercise, *Int. J. Numer. Meth. Fluids.* 3 (1982) 227-248.

[2] T. Fusegi and J. M. Hyun, Laminar and transitional natural convection in an enclosure with complex and realistic conditions, *Int. J. heat and fluid flow.* 15 (4) (1994) 258-268.

[3] J. M. Hyun, Unsteady buoyant convection in an enclosure, Advances in heat transfer. 24 (1994) 277-320.

[4] J. C. Patterson and S. W. Armfield, Transient features of natural convection in a cavity, *J. Fluid Mech.* 219 (1990) 469-497.

[5] M. R. Ravi, R. A. W. M. Henkes and C. J. Hoogendoorn, On the high-Rayleigh-number structure of steady laminar natural-convection flow in a square enclosure, *J. Fluid Mech.* 262 (1994) 325-351.

[6] J. C. Patterson and J. Imberger, Unsteady natural covection in a rectangular cavity, *J. Fluid Mech.* 100 (1980) 65-86.

[7] D. R. Chenoweth and S. Paolucci, Natural convection in an enclosed vertical air layer with large

horizontal temperature differences *J. Fluid Mech.* 169 (1986) 173-210.

[8] G. N. Ivey, Experiments on transient natural convection, *J. Fluid Mech.* 144 (1984) 389-401.

[9] J. S. Park and J. M. Hyun, Transient motion of a confined stratified fluid induced simultaneously by sidewall thermal loading and vertical through-flow, *J. Fluid Mech.* 451 (2002) 295-317.

[10] P. Luchini, Analytic and numerical solutions for natural convection in a corner, *AIAA J.* 24 (5) (1986) 841-848.

[11] S. G. Schladow, Oscillatory motion in a side-heated cavity, *J. Fluid Mech.* 213 (1990) 589-561.